

Non-perturbative solution of metastable scalar models

This article has been downloaded from IOPscience. Please scroll down to see the full text article.

2003 J. Phys. A: Math. Gen. 36 8703

(<http://iopscience.iop.org/0305-4470/36/32/310>)

View [the table of contents for this issue](#), or go to the [journal homepage](#) for more

Download details:

IP Address: 171.66.16.86

The article was downloaded on 02/06/2010 at 16:28

Please note that [terms and conditions apply](#).

Non-perturbative solution of metastable scalar models

Vladimír Šauli

Department of Theoretical Nuclear Physics, Nuclear Institute, Řež near Prague, Czech Republic

E-mail: sauli@ujf.cas.cz

Received 5 November 2002, in final form 17 June 2003

Published 29 July 2003

Online at stacks.iop.org/JPhysA/36/8703

Abstract

Dyson–Schwinger equations (DSEs) for propagators are solved for the scalar Φ^3 theory and massive Wick–Cutkosky model. With the help of integral representation, the results are obtained directly in Minkowski space in and beyond bare vertex approximation. Various renormalization schemes are employed which differ by the finite strength field renormalization function Z . The S -matrix is puzzled from the Green's function and the effect of truncation of the DSEs is studied. Independent of the approximation, the numerical solution breaks down for a certain critical value of the coupling constant, for which the on-shell renormalized propagator starts to develop the unphysical singularity at very high space-like square of momenta.

PACS numbers: 11.10.Gh, 11.15.Tk

1. Introduction

The Dyson–Schwinger equations (DSEs) are an infinite tower of the coupled integral equation relating Green's functions of the quantum field theory. If solved exactly, they could provide solutions of the underlying quantum field theory. In practice, the system of equations is truncated and we hope to obtain some information, in particular on the solution in the non-perturbative regime, from solving the simplest equation for the two-point Green's functions—the propagators. The other vertex functions, which also enter the DSE for the propagator, are either taken in their bare form or some physically motivated ansatz is employed.

In most papers dealing with the solution of DSEs, the Wick rotation from the Minkowski to Euclidean space is used to avoid singularities of the kernel inherent to the physical Green's functions. To our knowledge, the only exception is the series of papers [1–4] employing the so-called 'gauge technique' in quantum electrodynamics and its gauge invariant extension to quantum chromodynamics [5]; this work represents the birth of the 'pinch technique'. Until now, the above-mentioned approach has never been used in its non-perturbative context. Although not dealing with gauge theories, similarly to these techniques we instead solve directly in the momentum space, making use of the known analytical structure of the

propagator, expressed via the spectral decomposition. In the spectral or dispersive technique, we write the Green's function as a spectral integral over a certain weight function and denominator parametrizing known or assumed analytical structure. The generic spectral decomposition of the renormalized propagator reads

$$G(p^2) = \int d\alpha \frac{\tilde{\sigma}(\alpha)}{p^2 - \alpha - i\epsilon} \quad (1)$$

where $\tilde{\sigma}(\alpha)$ is called the Lehmann weight or simply the spectral function. If the threshold is situated above the particle mass, as it is for the stable (and unconfined) particles, then the spectral function typically looks like

$$\tilde{\sigma}(\alpha) = r\delta(m^2 - \alpha) + \sigma(\alpha) \quad (2)$$

where the singular delta function corresponds with non-interacting fields and σ appears due to the interaction. Finite parameters r then represent the propagator residuum and are simply related to field renormalization. It is also supposed that σ is a positive regular function which is spread smoothly from zero at the threshold. Note here that the positivity of Lehmann weight is not required for our solution, but the models studied in this paper naturally embodied this property; see, for instance, [6], or any standard textbook.

Putting the spectral decomposition of the propagators and the expression for the vertex function into the DSE allows us to derive the real integral equation for the weight function $\sigma(\alpha)$. This equation involves only one real principal value integration and can be solved numerically by iterations. Our solutions are obtained both for space-like and time-like propagator momenta; obtaining this in the Euclidean approach would require tricky backward analytical continuation. Since all momentum integration are performed analytically, there is no numerical uncertainty following from the renormalization which is usually present in Euclidean formalism [7]. Here, the renormalization procedure is performed analytically with the help of the direct subtraction in momentum space. This perturbative perfectly known renormalization scheme (see [8] for scalar models and [9] for the QED case, where a comparison with other perturbative renormalization schemes was also made) has been already applied to the QED and Yukawa model [10] in its non-perturbative context. In this paper, the off-shell momentum subtraction renormalization scheme was introduced and used. In order to simplify the technique and to compare various schemes we restrict ourselves to the choice of on-mass-shell subtraction point $\mu = m$.

In this work, we would like to present certain solutions of rather obscure theories: Φ^3 and $\Phi_i^2\Phi_j$ scalar models. The second model will be referred to here as the (generalized) Wick–Cutkosky model (WCM). In fact, not only models mentioned above but the all super-renormalizable four-dimensional scalar models are not properly defined since they have no true vacuum [11]. Instead of this they have only metastable vacua (here we assume non-zero masses of all particle content, in the opposite case the appropriate classical potential would not possess any local minimum). Instead of discarding these types of models, as sometimes happens, we look at whether this ‘inconsistency’ can be captured by the formalism of DSEs, or whether the appropriate solutions ‘behave ordinarily’. The property of super-renormalizability makes our models particularly suitable for this purpose. Actually, the super-renormalizability here implies the finiteness of the renormalization field constant Z which therefore cannot be considered at all (i.e. $Z = 1$). In the case of Φ^3 theory we do not fully omit the field renormalization but, with the help of the appropriate choice of the constant Z , we choose the given renormalization scheme. Making this explicitly and after the evaluation of the scattering amplitude, we look (in each scheme) at whether the observables do converge (in all schemes) to some experimentally measurable values of the virtual scalar world. As the suitable observables, we chose the amplitude M for the scattering process $\Phi\Phi \rightarrow \Phi\Phi$ and

we have not found any unexpected or even pathological behaviour. Instead of this, after the approximations of the full solutions improve, we will see that the amplitudes calculated in the various renormalization schemes tend to converge to each other; i.e. in this aspect, Φ^3 theory behaves as the ordinary and physically meaningful one. Here, this is the right place to note that the models with the metastable ground state serve as a useful methodological tool, the role in which they are often employed. In fact, Φ^3 theory serves as a good ground for the study of the various phenomena [12–15] (including phenomena such as non-perturbative asymptotic freedom and non-perturbative renormalization). There also exist a number of papers dealing with the WCM. The DSEs for propagators of the WCM in their simple bare vertex approximation have been solved for the purpose of calculating relativistic bound states [16] (for other recent work dealing with the bound-state problem within the WCM, see [17] and references therein). For the purpose of comparison with [16], we solve the exactly analogical Minkowski problem. The obtained value of the critical coupling should depend on the renormalization scheme. Having this slight dependence under control, it allows us to compare with other non-perturbative methods [18, 19]. The comparison with conventional perturbation theory is also made.

Regardless of the facts mentioned above, we are far from concluding that the Φ^3 model is a fully physically satisfactory one, since we do not know anything about the full solution. At this point, the study presented in this paper and the studies of the Φ^3 model in five [12] and six [13] dimensions are conclusive in a similarly cautious way. Probably, a more sophisticated conclusion could be obtained by some lattice study, which has not yet been done for this purpose.

At the end of the introduction, we should mention that there is always the possibility of including a sophisticated cut-off function $f(\Lambda)$ into the Lagrangian and to regard our cubic models as an effective model below this cut-off. The theory at energies above Λ could be another field theory or string theory, or whatever. However, this method is developed and the appropriate Polchinski renormgroup equations may be written down [20, 21]. These cut-off methods lie somehow beyond the scope of this paper and we prefer to use the usual renormalization schemes, where the independence on the appropriate regularization procedure is manifest. Clearly, with the use of the cut-off method it would be difficult to perform the aforementioned comparison with the results [16], where the on-mass-shell renormalization scheme has been performed. Furthermore, we should note here that the dispersion technique used throughout the proposed paper would become more complicated due to the presence of the profile function $f(\Lambda)$.

In the next section we present the DSEs for Φ^3 for propagator and vertex functions. Subsequently we discuss the renormalization procedure and rewrite the propagator equation in its spectral form. Also, the numerical results and limitations are discussed. The WCM is dealt with in section 3. It is solved numerically in its pure bare vertex approximation. The details of calculations are relegated to appendices A and B.

2. Φ^3 theory

2.1. Dyson–Schwinger equation for Φ^3 theory

The Lagrangian density for this model reads

$$\mathcal{L} = \frac{1}{2} \partial_\mu \phi_0(x) \partial^\mu \phi_0(x) - \frac{1}{2} m_0^2 \phi_0^2(x) - g_0 \phi_0^3(x) \quad (3)$$

where index 0 indicates the unrenormalized quantities. With the help of the functional differentiation of a generating functional (for this procedure, see for instance [22]) with

classical action determined by equation (3) we obtain the following DSE (after transforming into the momentum space) for the inverse propagator

$$\begin{aligned} G_0^{-1}(p^2) &= p^2 - m_0^2 - \Pi_0(p^2) \\ \Pi_0(p^2) &= i3g_0 \int \frac{d^4q}{(2\pi)^4} \Gamma_0(p-q, q) G_0(p-q) G_0(q) \end{aligned} \quad (4)$$

where Γ_0 is the full irreducible three-point vertex function which satisfies its own DSE (10). The integral of Π_0 is divergent and requires the mass renormalization. Making the on-mass-shell subtraction we define renormalized self-energy Π_{R1}

$$\Pi_{R1}(p^2) = \Pi_0(p^2) - \Pi_0(m^2) \quad (5)$$

where m is the pole 'physical' mass, given by the equation $G^{-1}(m^2) = 0$. Defining the mass counter-term

$$m^2 = m_0^2 - \delta m^2 \quad \delta m^2 = \Pi_0(m^2) \quad (6)$$

and introducing additional finite renormalization constant

$$\phi_0 = \sqrt{Z}\phi \quad g_0 = g \frac{Z_g}{Z^{\frac{3}{2}}} \quad (7)$$

we obtain the inverse of the full propagator in term of physical mass

$$\begin{aligned} G^{-1}(p^2) &= Z(p^2 - m^2) - \Pi_1(p^2) \\ \Pi_1(p^2) &= Z(\Pi_0(p^2) - \Pi_0(m^2)) \\ Z\Pi_0(p^2) &= i3g^2 \int \frac{d^4q}{(2\pi)^4} \Gamma(p-q, q) G(p-q) G(q) \end{aligned} \quad (8)$$

where g is a renormalized coupling and the constant Z_g corresponds to the renormalization of the vertex function, and G represents the renormalized propagator with respect to the field strength renormalization, i.e.

$$\Gamma = Z_g \Gamma_0 \quad G_0(p^2) = ZG(p^2). \quad (9)$$

We closed the system of DSEs already at the level of equation for proper vertex. Instead of solving the full renormalized DSE for the vertex

$$g\Gamma(p, l) = 6g + 6gi \int \frac{d^4q}{(2\pi)^4} \Gamma(p, q) G(q) G(l-q) M(q, l, p) \quad (10)$$

we approximate it by the first two terms of the appropriate skeleton expansion

$$g\Gamma(p, l) = 6g + i(6g)^3 \int \frac{d^4q}{(2\pi)^4} G(q) G(p-q) G(l-q) \quad (11)$$

i.e. we approximate the vertex inside the loop by its bare value and the scattering matrix M in equation (10) is taken in its dressed tree approximation, i.e. $M = G$. In the following, we use the name *dressed vertex* (DV) or improved approximation for the solution of the propagator when equation (11) is used for obtaining the triplet scalar vertex Γ and in the same spirit we use the name *bare vertex* (BV) approximation for such a solution where only the bare vertex was used. The improvement of the approximation is achieved by the skeleton expansion of the proper Green's function where the series of DSEs is thrown away. Here, this is done at the level of the triplet vertex. In [23], we can see how the problem is becoming more complicated when M is non-trivially taken into account.

The equation for the propagator is solved in BV and DV approximations at each renormalization scheme separately. We define these in the following section.

2.2. Choosing the scheme

We assume (or rather we neglect it) that there interaction does not create the bound states contributing to the weight function σ . We use the name *minimal momentum subtraction* renormalization scheme (MMS) where the only mass subtraction is used and where the field leaves unrenormalized, i.e. $Z = 1$. Therefore, we can write the spectral decomposition for the propagator and for the self-energy Π in the following form

$$\begin{aligned}
 G(p^2) &= \frac{r}{p^2 - m^2} + \int_{4m^2}^{\infty} d\alpha \frac{\sigma(\alpha)}{p^2 - \alpha - i\epsilon} \\
 &= \{p^2 - m^2 - \Pi_1(p^2)\}^{-1} \\
 \Pi_1(p^2) &= \int_{4m^2}^{\infty} d\alpha \frac{\rho(\alpha)(p^2 - m^2)}{(\alpha - m^2)(p^2 - \alpha + i\epsilon)}
 \end{aligned} \tag{12}$$

where $\pi\rho(s)$ represents the self-energy absorptive part and the threshold value of momentum $P_t^2 = 4m^2$ is explicitly written. Obviously, in this MMS the propagator does not have the pole residue r equal to unity

$$\begin{aligned}
 \lim_{p^2 \rightarrow m^2} (p^2 - m^2)G(p^2) &= \left[1 - \frac{d}{dp^2} \Pi_1(p^2) \Big|_{p^2=m^2} \right] = r \\
 \frac{d}{dp^2} \Pi_1(p^2) \Big|_{p^2=m^2} &= \int_{4m^2}^{\infty} d\alpha \frac{-\rho(\alpha)}{(\alpha - m^2)^2}.
 \end{aligned} \tag{13}$$

After a simple algebra and taking the imaginary part of equation (12) we arrive at the relation between the spectral functions σ and ρ

$$\sigma(\omega) = \frac{r\rho(\omega)}{(\omega - m^2)^2} + \frac{1}{\omega - m^2} P. \int_{4m^2}^{\infty} d\alpha \frac{\sigma(\omega)\rho(\alpha)\frac{\omega-m^2}{\alpha-m^2} + \sigma(\alpha)\rho(\omega)}{\omega - \alpha} \tag{14}$$

where $P.$ denotes principal value integration.

This is the first of two necessarily coupled equations which we actually solve for a given theory. We discuss it in some detail since its form depends only on the adopted renormalization procedure, not on the actual form of the interaction, nor on the approximation employed for the vertex function Γ in the DSE for the propagator. The second equation connecting σ and ρ does depend on the form of vertex. Its derivation is more complicated and we deal with it in appendix A.

In some cases, the form (14) is not the most convenient one; for instance, when we want to look the bound-state spectrum influence causes just by the self-energy effect [24]. Note the presence of the constant r in the first term on the right-hand side; it has to be determined from the relations (13) after each iteration. To get rid of this, we define the usual *on-shell renormalization scheme with unit residuum* (OSR scheme) by

$$Z = 1 + \delta Z \quad \delta Z = \frac{d}{dp^2} \Pi_1(p^2) \Big|_{p^2=m^2} \tag{15}$$

which gives the standard receipt how to calculate the OSR propagator

$$\begin{aligned}
 G^{\text{OSR}}(p^2) &= \{p^2 - m^2 - \Pi_2(p^2)\}^{-1} \\
 \Pi_2(p^2) &= \Pi(p^2) - \Pi(m^2) - \frac{d}{dp^2} \Pi(p^2) \Big|_{p^2=m^2} (p^2 - m^2) \\
 \Pi(p^2) &= i3g_2^2 \int \frac{d^4q}{(2\pi)^4} \Gamma(p - q, q)G(p - q)G(q)
 \end{aligned} \tag{16}$$

and subsequently implies the spectral decomposition for G^{OSR} and Π_2

$$\begin{aligned} G^{\text{OSR}}(p^2) &= \frac{1}{p^2 - m^2} + \int_{4m^2}^{\infty} d\alpha \frac{\sigma_2(\alpha)}{p^2 - \alpha - i\epsilon} \\ \Pi_2(p^2) &= \int_{4m^2}^{\infty} d\alpha \frac{\rho_2(\alpha)(p^2 - m^2)^2}{(\alpha - m^2)^2(p^2 - \alpha + i\epsilon)}. \end{aligned} \quad (17)$$

The relation between σ_2 and ρ_2 is now derived in the same way as before and it reads

$$\sigma_2(\omega) = \frac{\rho_2(\omega)}{(\omega - m^2)^2} + \frac{1}{\omega - m^2} P \cdot \int_{4m^2}^{\infty} d\alpha \frac{\sigma_2(\omega)\rho_2(\alpha)\left[\frac{\omega - m^2}{\alpha - m^2}\right]^2 + \sigma_2(\alpha)\rho_2(\omega)}{\omega - \alpha}. \quad (18)$$

Note that equations (14) and (18) are inequivalent due to the scheme difference. The appropriate dependence of the weights ρ and ρ_2 on the coupling constants g and g_2 is explicitly written in appendices A and B, respectively. (Two inequivalent renormalization schemes should give different Green's functions, but should give the same S -matrix.)

At the end of this section, we very briefly discuss dimensional renormalization prescription [25], showing here that it is fully equivalent to MMS to all orders (note that the perturbation theory is naturally generated by the coupling constant expansion of the DSE's solution). For this purpose we choose the *modified minimal subtraction* $\bar{M}S$ scheme, noting that any other sort of scheme based on the dimensional regularization method would be treated in the same way. Since the only infinite contributions are affected when this renormalization is applied, therefore the contribution with the dressed vertex (master diagram and so that) satisfies the unsubtracted dispersion relation (DR) while for instance the one-loop skeleton self-energy diagram (in a fact the only irreducible contribution which is infinite in four dimensions) looks (for space-like momenta) like

$$\Pi_{\bar{M}S}^{[1]}(p^2) = \frac{18g^2}{(4\pi)^2} \int_0^1 dx \ln \left\{ \frac{m^2 - p^2 x(1-x)}{\mu_{\text{t'Hooft}}^2} \right\} + \Pi(p^2)_{\text{finite}} \quad (19)$$

where Π_{finite} represents the omitted finite terms which are not affected by dimensional renormalization at all (since they are finite to all orders).

The inverse of the full propagator reads in this scheme

$$G_{\bar{M}S}^{-1}(p^2) = p^2 - m^2(\mu_{\text{t'Hooft}}) - \Pi_{\bar{M}S}^{[1]}(p^2) - \Pi(p^2)_{\text{finite}}. \quad (20)$$

Identifying the pole mass by equality $G_{\bar{M}S}^{-1}(p^2 = m_p^2) = 0$ we simply arrive at the result

$$G_{\bar{M}S}^{-1}(p^2) = p^2 - m_p^2 - \Pi_1(p^2) \quad (21)$$

where

$$\begin{aligned} m_p^2 &= m^2(\mu_{\text{t'Hooft}}) + \Pi_{\bar{M}S}^{[1]}(m_p^2) + \Pi(m_p^2)_{\text{finite}} \\ \Pi_1(p^2) &= \Pi_{\bar{M}S}^{[1]}(p^2) - \Pi(p^2)_{\text{finite}} - \Pi_{\bar{M}S}^{[1]}(m_p^2) - \Pi(m_p^2)_{\text{finite}}. \end{aligned} \quad (22)$$

Since the pole mass is a renormgroup invariant quantity, we see that the $\bar{M}S$ scheme exactly corresponds with the single-subtraction renormalization scheme, i.e. the MMS. Note here that in renormalizable models such identification is not so straightforward but always possible [9]. Of course, the appropriate identification is then rather complicated. To conclude this section, we can see that the popular renormalization prescription such as MS or $\bar{M}S$ schemes can be ordinarily used in the non-perturbative context. At this point we disagree with the opposite statement of the paper [28].

2.3. Test of scheme (in-)dependence

The physical observables should be invariant not only with respect to the choice of renormalization scale, but also with respect to the choice of renormalization scheme. The first invariance is more than manifest in our approach, since all the quantities used here are the renormgroup invariants. The second mentioned invariance is less obvious and, in fact, it is clear only for some very simple cases. (The most simple case is the tree-level amplitude evaluation, where the residua of the propagators may be exactly absorbed into the redefinitions of the coupling constants; but, of course, in this case the renormalization is not required.) In any reasonable renormalizable quantum field theory, it is strongly believed that the obtained exact Green’s functions must build the same S -matrix. In perturbation theory, we usually have several first terms of perturbation expansion and we hope that they offer a satisfactory description of the nature when the ‘right’ choice of renormalization scheme is made [9, 26]. Furthermore, we should be aware that the possible sum of infinitely many terms of perturbation series should be regarded as an asymptotic one. In fact, the application of some sophisticated resummation technique is necessary in that case [22, 27].

In DSE treatment we can talk about the level of DSE’s system truncation instead of a given coupling order. In the text below we describe a simple possible procedure of how to see the improvements of a physical observable when it is calculated within the improved truncation of DSEs. For this purpose, the BV and DV solutions of DSEs in both MMS and OSR schema are used to compose the same physically measurable quantity.

For our explanation we have explicitly chosen the matrix element M of the elastic scattering process $\phi\phi \rightarrow \phi\phi$ which can be written

$$M(s, t, u) = \sum_{a=s,t,u} \Gamma G(a)\Gamma + \dots = \sum_{a=s,t,u} (6g)^2 G(a) + \dots \tag{23}$$

The dots denote neglected boxes and crossed boxes contributions and the letters s, t, u in equation (23) represent the usual Mandelstam variables that satisfy $s + t + u = 4m^2$, since now, the external particles are on-shell.

Using the notations introduced in the previous section, then the matrix M in MMS scheme is calculated as

$$M^{\text{MMS}} = \sum_{a=s,t,u} (6g)^2 G(a) \tag{24}$$

where the propagator is calculated through equations (12), (13) and(14). For OSR, the scattering matrix is composed as

$$M^{\text{OSR}} = \sum_{a=s,t,u} (6g_2)^2 G_{\text{OSR}}(a) \tag{25}$$

where the propagator is calculated through equations (16), (17) and (18) and the relations for ρ are reviewed in appendices A and B.

In the ideal case we would obtain

$$M_{\text{MMS}} = M_{\text{OSR}} \tag{26}$$

which should be a consequence of exact scheme independence. In reality, relation (26) is not exactly fulfilled due to the truncation of the DSE system. In what follows, we describe how to check the consistent condition (26) and how to see the appropriate deviation numerically.

Clearly, the equality should be valid in each kinematic channel separately. For instance, choosing the t -channel for this purpose and comparing the pole part of matrices M we obtain

the relation between the coupling at each scheme

$$g_2^2 = r g^2 \quad (27)$$

where r is the residuum calculated from equation (13). This implies for us that if we calculate the Green's function in the OSR scheme to compose the same S -matrix the Green's functions in the MMS scheme must be calculated with the coupling $g_2 = \sqrt{r}g$. Having the results for σ and σ_2 extracted from the DSEs solved in the appropriate schemes, we can compare imaginary parts of scattering matrices M_{MMS} and M_{OSR} . Our approximation (24) and (25) implies

$$g_2^2 \sigma_2(\omega) = g^2 \sigma(\omega). \quad (28)$$

How accurately this equality is fulfilled at non-trivial regime $t > 4m^2$ can be simply checked. For this purpose we evaluate the integral (weighted) deviation E_N

$$\begin{aligned} E_N &= \frac{\int [M_{\text{OSR}}(t) - M_{\text{MMS}}(t)] \frac{dt}{t^N}}{\int [M_{\text{OSR}}(t) + M_{\text{MMS}}(t)] \frac{dt}{t^N}} \\ &= \frac{\int [\sigma_2(t) - \sigma(t)/r] \frac{dt}{t^N}}{\int [\sigma_2(t) + \sigma(t)/r] \frac{dt}{t^N}} \end{aligned} \quad (29)$$

where the parameter N serves to adjust the regime of momenta in which we are interested. A larger value of N enhanced the threshold values of momenta while the ultraviolet modes are suppressed in that case. We choose $N = 0, 1$ for the purpose of this paper.

Let us stress at the end of this section, that the next leading order of M is scheme-invariant and all the differences therefore follow from the remnant of the full DSE solution. Hence only negligible deviation is expected for small couplings. Also, in general, the deviation E_N should decrease when considered approximations become more and more close to the full non-perturbative solution and it should principally vanish for the exact solution. In other words, E_N must decrease when the approximation (truncation of DSEs) improves. The results obtained by the above sketched method are reviewed in the next section.

2.4. Results

The integral equations for Lehmann weights have been solved numerically by the method of iteration. The appropriate solutions, obtained for several hundreds of mesh points and with the use of some sophisticated integrator, have an accuracy of approximately one part of 10^4 for a reasonable value ($\lambda \ll \lambda_{\text{crit}}$) of the coupling strength λ and increase (up to several per cent) when $\lambda \simeq \lambda_{\text{crit}}$. The coupling strength is defined as dimensionless quantity

$$\lambda = \frac{18g^2}{16\pi^2 m^2}. \quad (30)$$

The critical value of λ is simply defined by the collapse of the (numerically sophisticated) solution of the imaginary part DSEs. Before making a comparison of physical quantities, we present the numerical results for the Green's functions. In figure 1 the so-called dynamical mass

$$M(p^2) = G^{-1}(p^2) - p^2 \quad (31)$$

of the Φ^3 theory boson is presented for various coupling strengths in both renormalization schemes. The infrared details are displayed in figure 2. The dynamical mass is not directly physically observable since it is scheme-dependent from the definition; the exception is the pole mass which is scheme-independent and renormgroup-invariant as well. It is interesting

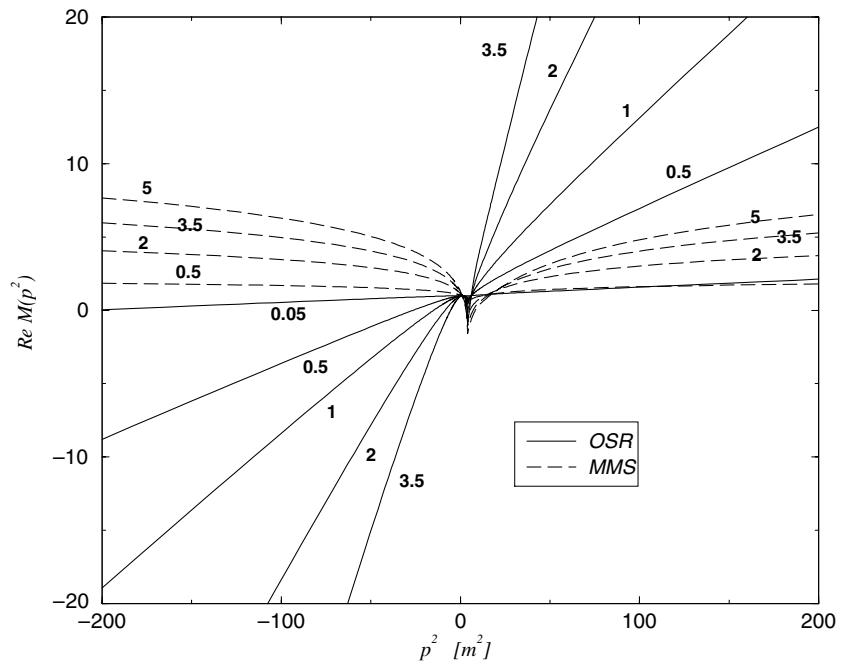


Figure 1. Dynamical mass of scalar particle in Φ^3 theory calculated in the bare vertex approximation in both renormalization schemes. The lines are labelled by λ_{MMS} for the MMS scheme and λ_{OSR} for the OSR renormalization scheme.

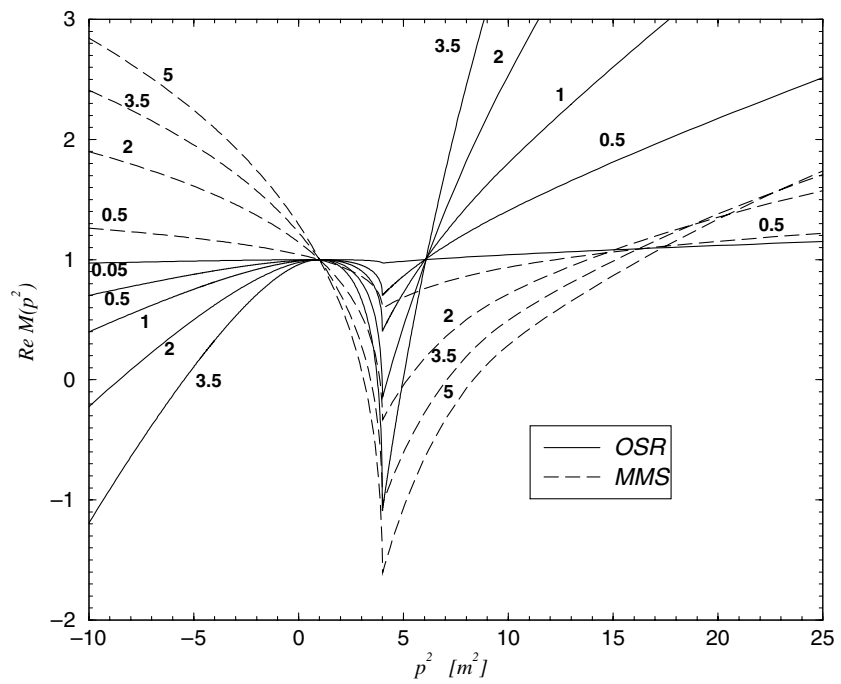


Figure 2. Infrared (threshold) details of figure 1.

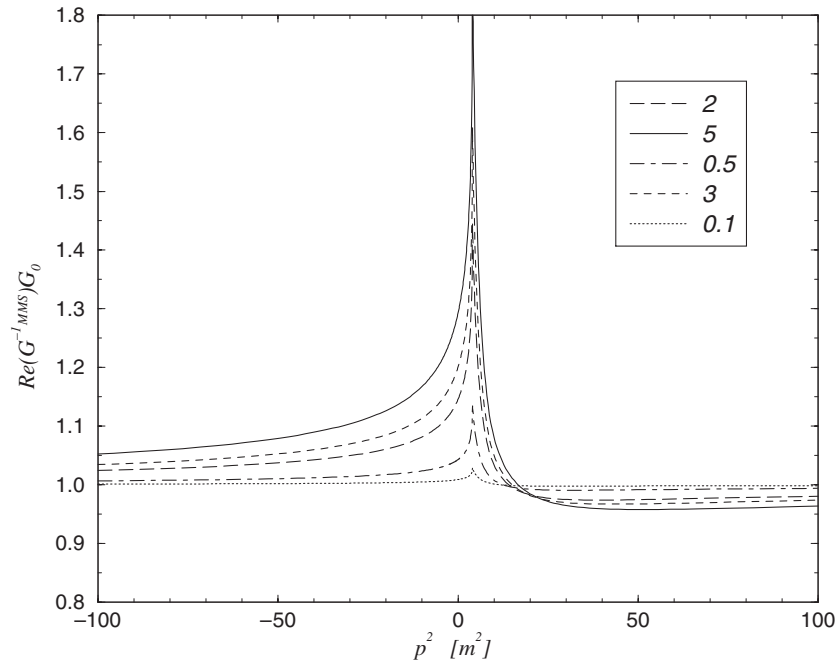


Figure 3. The propagator deviations from free theory. The propagator is calculated in minimal momentum renormalization scheme for various λ_{MMS} .

that there are time-like values of square of momenta where the propagators behave almost like free ones, no matter how strong the coupling constant. This occurs somewhere around the point $p_f^2 = 6m^2$ for the OSR scheme and approximately at $p_f^2 = 20m^2$ for the MMS scheme, which implies the physical irrelevance of such a behaviour. (Of course, there are always differences within the absorptive parts $\pi\rho$ which are ordinarily coupling constant dependent at these points.) The appropriate relevance of propagator dressing is best seen when the dressed propagator is compared with the free one $G = (p^2 - m^2)^{-1}$. From figures 3 and 4, we can see that the propagator function is the most sensitive with respect to the self-energy correction for threshold momenta where these correction are enhanced about one magnitude, while they are largely suppressed for the above-mentioned values of momenta p_f^2 . Note that nothing from these facts can be read from the purely Euclidean approach. The results presented up to now have been calculated in the bare vertex approximation; the solution with vertex correction included will be discussed below. The appropriate bare vertex approximation critical coupling value is $\lambda_{\text{crit}}^{\text{OSR}} \simeq 3.5$ for the OSR scheme and $\lambda_{\text{crit}}^{\text{MMS}} \simeq 5$ for the MMS scheme. Their different values are not a discrepancy but the necessary consequence of the renormalization scheme dependence.

Furthermore, in order to see the effect of self-consistency of the DSE treatment we compare the DSE result with the perturbation theory in the OSR scheme. From figure 5 we can see that the perturbation theory is perfectly suited method when applied somewhere below the critical value of the coupling. Therefore, the main goal of our solution is the information about the domain of validity of the given model.

The issue of vertex improvement by the one-loop skeleton diagram and its appropriate effect on the DSE solution and scattering matrix is discussed in the text below. First let us note that the critical values of the couplings decrease and we have $\lambda_{\text{crit}}^{\text{dressed vertex}} \simeq \lambda_{\text{crit}}^{\text{bare vertex}}/2$,

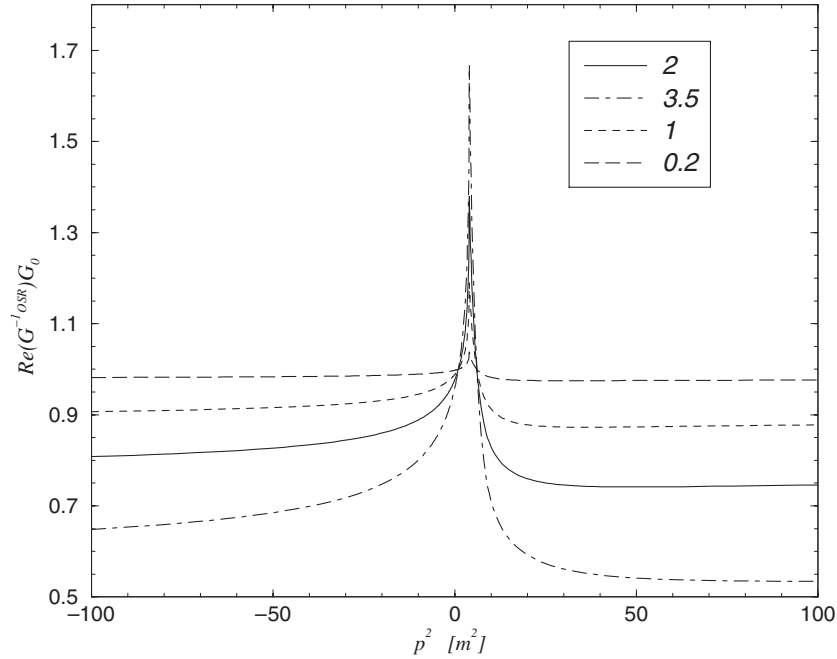


Figure 4. The propagator deviation from free theory. The propagator is calculated in the on-mass-shell renormalization scheme with unit residuum for various λ_{OSR} .

which is roughly valid for both renormalization schemes employed. We return to the question of meaning λ_{crit} when we discuss the WCM.

To make our comparison of the proposed methods more meaningful, we do not compare the Green's functions but rather we look at the scattering amplitudes M calculated in both renormalization schemes obtained in both truncations of DSEs. In figure 6 we compare the imaginary parts of scattering amplitudes M at a given kinematic channel. The comparison is made in the way proposed and described in the previous section. Henceforth, what are actually compared in this figure are the Lehmann weights σ of the MMS scheme calculated for certain λ_{MMS} and the rescaled Lehmann weights $r\sigma_2$ calculated for the OSR scheme with the appropriate coupling strength $\lambda_{\text{OSR}} = r\lambda_{\text{MMS}}$. It is then apparent that the lines for $\text{Im } M_{\text{OSR}}(r\lambda_{\text{MMS}}, t)$ and $\text{Im } M_{\text{MMS}}(\lambda_{\text{MMS}}, t)$ for solutions with dressed vertices are much closer each other than the solution with bare vertices. This statement is valid for all t for a given theory characterized by its coupling constant (with λ_{MMS} fixed). This is true for all couplings λ , the only—but not so striking—exception is certain infrared excess for the value of couplings close to the critical one. Of course, the worse numerical accuracy plays a role in strong coupling. Nevertheless, we can see that when the approximation improves then there is apparent signal for achieving the renormalization scheme independence for all values of the coupling constant.

In order to see the aforementioned quantitative improvement we have calculated the appropriate deviations E_N and $N = 0, 1$. The results for some larger value of the couplings are presented in table 1. The corresponding difference becomes negligible when λ decreases and approaches its 'perturbative' value. For better orientation the infrared details for three choices of the coupling constants are also displayed in figure 7.

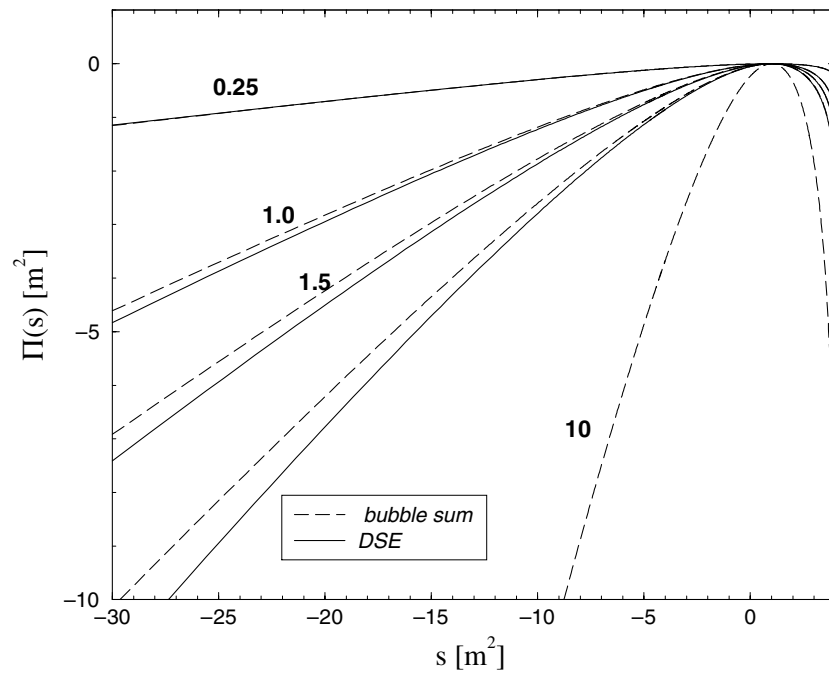


Figure 5. Comparison of DSE results in the bare vertex approximation with the perturbation theory result. DSE and bubble summation is compared in the OSR scheme. Each two close lines of different types correspond to the same value of coupling $\lambda_{OSR} = \{0.25; 1.0; 1.5; 2.2\}$. The lowest dashed line with $\lambda = 10$ does not have its DSE partner solution (since $\lambda > \lambda_c$).

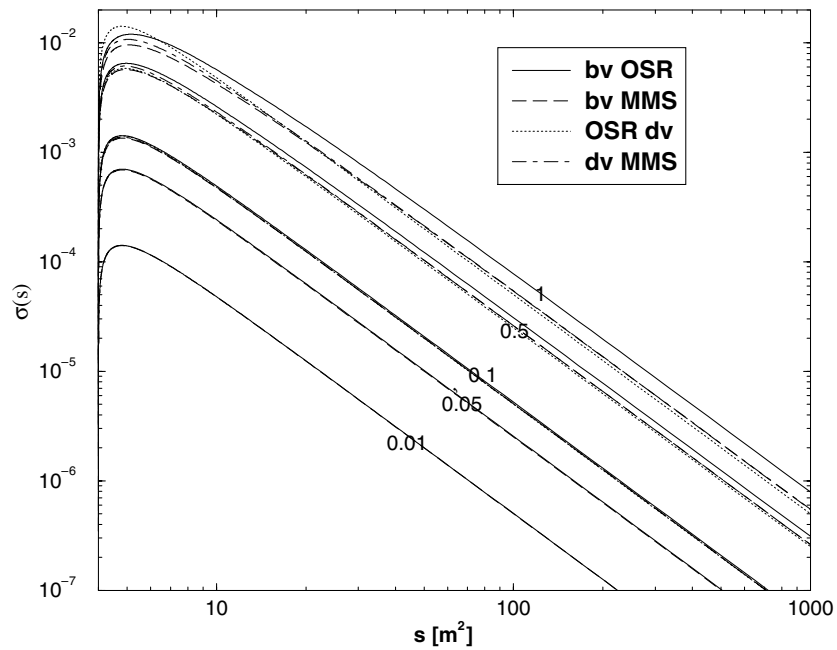


Figure 6. Imaginary parts of the scattering matrix calculated with a propagator which have been obtained in the MMS and OSR schemes with (dv) and without (bv) an improved vertex. Each set of lines corresponding to the same model is labelled by the coupling strength λ_{MMS} .

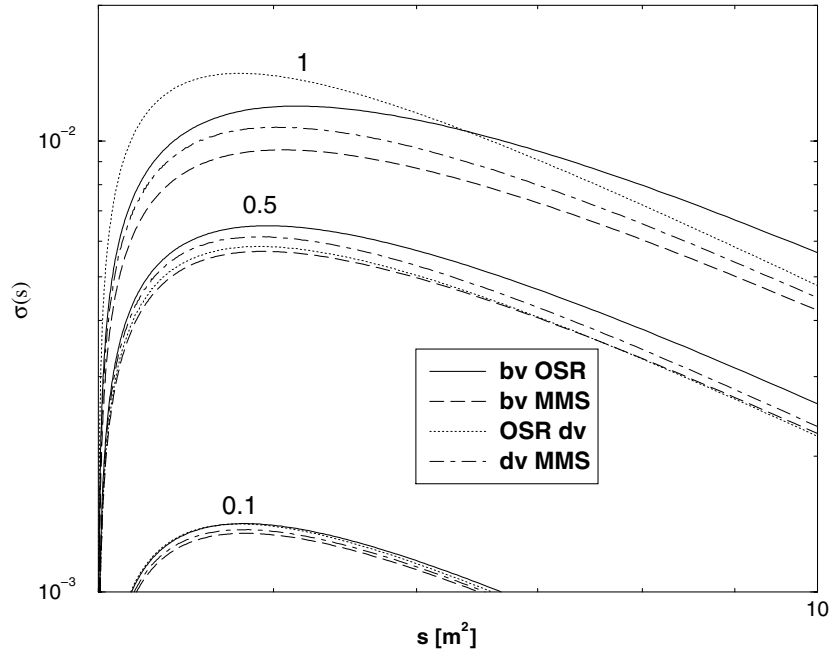


Figure 7. The low-frequency details of figure 6.

Table 1. Normalized and weighted integral deviations E_N between scattering amplitudes calculated in the OSR and MMS schemes. Exact scheme independence corresponds to the case $E_N = 0$. The parameter $N = 1$ makes the quantity E more sensitive to the systematic error in the infrared domain. The notation BV(DV) means that the appropriate propagator was calculated with a bare (dressed) vertex. The function E is displayed for three cases of results presented in figures 6 and 7.

	$E_{N=0}$ BV	$E_{N=0}$ DV	$E_{N=1}$ BV	$E_{N=1}$ DV
$\lambda = 0.1$	0.020	0.0039	0.022	0.0078
$\lambda = 0.5$	0.076	0.025	0.071	0.025
$\lambda = 1.0$	0.15	0.040	0.13	0.08

3. DSEs for the WCM

The massive WCM is given by the following Lagrangian

$$\mathcal{L} = \sum_i \frac{1}{2} \partial_\mu \Phi_i \partial^\mu \Phi_i - \sum_i \frac{1}{2} m_i^2 \Phi_i^2 + \left(\frac{g_{13}}{\sqrt{2}} \Phi_1^2 + \frac{g_{23}}{\sqrt{2}} \Phi_2^2 \right) \Phi_3 + \text{C.P.} \quad (32)$$

where C.P. means the appropriate counter-term part. Here we choose the second renormalization scheme employed in the previous section, i.e. the propagators of all three particles have the unit residua. All the definitions of counter-terms δZ_i , δm_i , δg_i correspond with the OSR defined previously but now for each particle separately. Furthermore, we adjust the couplings to be

$$g_{i3} = \frac{Z_{g_{i3}}}{Z_i Z_3^{\frac{1}{2}}} g_{i3_0} \quad i = 1, 2 \quad (33)$$

such that

$$g_{13} = g_{23}. \quad (34)$$

The equal mass case $m_1 = m_2$ has already been solved [24] for the purpose of studying the self-energy effect on the bound-state spectrum. Here we solve the unequal mass case

$$\frac{m_1}{m_2} = 4 \quad m_3 = m_2 \quad (35)$$

and compare the result with the Euclidean version of solution [16]. We restrict ourselves to the bare vertex approximation which is sufficient for comparison with [16]. Since all the derivation is rather straightforward, we simply review the results. The renormalized DSEs in bare vertex approximation read

$$\begin{aligned} G_{Ri}^{-1}(p) &= p^2 - m_i^2 - \Pi_{i(2)}(p^2) \quad i = 1, 2 \\ G_{R3}^{-1}(p) &= p^2 - m_3^2 - \Pi_{3(2)}(p^2) \\ \Pi_i(p^2) &= i2g^2 \int \frac{d^4q}{(2\pi)^4} G_3(p-q)G_i(q) \quad i = 1, 2 \\ \Pi_3(p^2) &= ig^2 \int \frac{d^4q}{(2\pi)^4} \sum_{i=1,2} G_i(p-q)G_i(q) \end{aligned} \quad (36)$$

where the bracketed index denotes the renormalization scheme employed, and the second index labels the particle associated with the appropriate field in the Lagrangian (32). All the propagators satisfy the Lehmann representation with unit residuum and all the proper function obeys the double-subtracted DR (17). Henceforth, the appropriate spectral weights are related through the relations

$$\sigma_i(\omega) = \frac{\rho_i(\omega)}{(\omega - m_i^2)^2} + \frac{1}{(\omega - m_i^2)} P. \int_{(m_j+m_k)^2}^{\infty} d\alpha \frac{\sigma_i(\omega)\rho_i(\alpha) \left[\frac{\omega - m_i^2}{\alpha - m_i^2} \right]^2 + \sigma_i(\alpha)\rho_i(\omega)}{\omega - \alpha} \quad (37)$$

where for the indices $i = 1, 2$ we have $j = 2, 3; k = 3, 3$ and for particle three the index $j = k = 2$ since it labels the lighter particle with the mass m_2 . The expression for the absorptive parts is

$$\begin{aligned} \rho_{\pi_i}(\omega) &= \frac{2g^2}{(4\pi)^2} \left[B(m_i^2, m_3^2; \omega) + \int_0^{\infty} d\alpha (B(\alpha, m_i^2; \omega)\sigma_3(\alpha) + B(\alpha, m_3^2; \omega)\sigma_i(\alpha)) \right. \\ &\quad \left. + \int_0^{\infty} d\alpha d\beta B(\alpha, \beta; \omega)\sigma_3(\alpha)\sigma_i(\beta) \right] \quad i = 1, 2 \\ \rho_{\pi_3}(\omega) &= \sum_{i=1,2} \frac{g^2}{(4\pi)^2} \left[\sqrt{1 - \frac{4m_i^2}{\omega}} + 2 \int_0^{\infty} d\alpha B(\alpha, m_i^2; \omega)\sigma_i(\alpha) \right. \\ &\quad \left. + \int_0^{\infty} d\alpha d\beta B(\alpha, \beta; \omega)\sigma_i(\alpha)\sigma_i(\beta) \right] \end{aligned} \quad (38)$$

where we freely integrate over the the whole range of positive real axis leaving the information about the appropriate thresholds and subthresholds absorbed in the definition of the function B .

The above set of equations has actually been solved numerically. The main result for us is the appearance of the critical coupling strength $\lambda_c \equiv g_c^2 / (4\pi m_2^2) = 0.12$ which rather accurately corresponds with the point where the renormalization constant Z_2 turns out to be

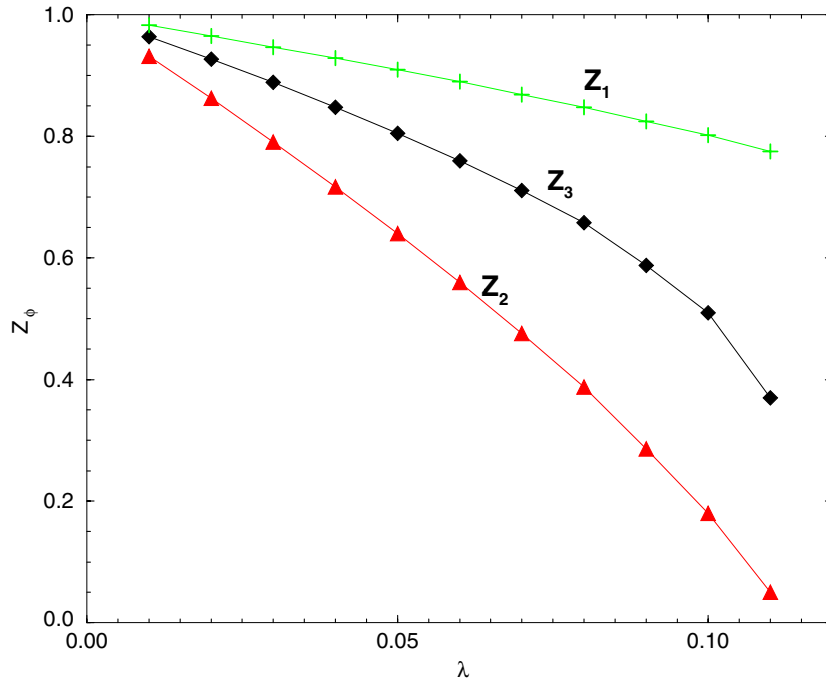


Figure 8. The dependence of field strength renormalization constants on the coupling strength of the WCM. The indices 1–3 label the particles.

negative. The appropriate dependence of the renormalization constants Z_i is presented in figure 8 for all three particles. The obtained critical value is in reasonable agreement with that obtained by the Euclidean solution of the DSE system [16], where $\lambda_c = 0.086$, as well as with the critical value $\lambda_c = 0.063$ which was found using a variational approach [18, 19].

Furthermore, the existence of the critical coupling of OSR scheme can be seen from the analytical formula for the inverse of propagator

$$G_i^{-1} = p^2 - m_i^2 - \int_0^\infty d\alpha \frac{\rho_i(\alpha)(p^2 - m_i^2)^2}{(\alpha - m_i^2)^2(p^2 - \alpha + i\epsilon)} \quad (39)$$

which implies that for strong enough coupling the Landau pole should appear, which must arise when the factor L

$$L = \left[1 - \int_0^\infty \frac{\rho(\alpha)}{(\alpha - m^2)^2} \right] \quad (40)$$

is negative (when it is just zero then the Landau pole is situated in space-like infinity, and for the positive L this singularity never appears due to the finiteness of the appropriate integral in equation (40)). For negative L the propagator cannot satisfy Lehmann representation at all and at least the Minkowskian treatment used in this work must fail. Comparing equation (40) with the definition of renormalization constant Z we clearly have the identification $L = Z$. As we have mentioned, the numerical solution starts to fail when the condition $Z = 0$ is fulfilled. This statement is justified with 10% numerical accuracy. (We have no similar guidance for the MMS scheme but we expect the similar appearance of the critical coupling λ_{MMS} for this scheme, as occurred in Φ^3 theory, but the reason for the numerical failure in this case is not found in this paper.)

4. Conclusion

We have obtained numerical solutions of the DSEs in Minkowski space for Φ^3 theory and the WCM. This suggests that the expansion of the theory around the metastable vacuum leads to the predicative result. Our technique allows us to extract propagator spectral function $\rho(s)$ with reasonably high numerical accuracy. Since the renormalization procedure is performed analytically, it has no effect on the precision of the solution. When the coupling does not exceed a certain critical value, then the domain of analyticity of the propagator is the all real axis of p^2 . An attempt to clarify the meaning of the critical coupling value was made. This suggests that it corresponds with the appearance of unphysical singularity in the on-shell renormalized propagator. Consequently, the field renormalization constant (in the on-shell scheme) turns to be negative for $\lambda > \lambda_{\text{crit}}$.

Appendix A. Dispersion relations for self-energies in bare vertex approximation

In this appendix we derive DRs for self-energies in both renormalization schemes for the bare vertex. The calculation is very straightforward, and in fact it represents nothing but an evaluation of the one-loop scalar Feynman diagram with different masses in internal lines.

Substituting the Lehmann representation for MMS propagators (12) the unrenormalized Π can be split as

$$\begin{aligned}\Pi(p^2) &= \Pi_{(b,b)}(p^2) + 2\Pi_{(b,s)}(p^2) + \Pi_{(s,s)}(p^2) \\ \Pi_{(b,b)}(p^2) &= \int d\bar{q} \frac{18r^2g^2}{((p+q)^2 - m^2 + i\epsilon)(q^2 - m^2 + i\epsilon)} \\ \Pi_{(b,s)}(p^2) &= \int d\bar{q} \int d\alpha \frac{18rg^2\sigma(\alpha)}{(q^2 - \alpha + i\epsilon)((p+q)^2 - m^2 + i\epsilon)} \\ \Pi_{(s,s)}(p^2) &= \int d\bar{q} \int d\alpha d\beta \frac{18g^2\sigma(\alpha)\sigma(\beta)}{((p+q)^2 - \alpha + i\epsilon)(q^2 - \beta + i\epsilon)}\end{aligned}\tag{A.1}$$

where we have used shorthand notation for the measure $i d^4q/(2\pi)^4 \equiv d\bar{q}$. Making the subtraction, we immediately arrive for the pure perturbative contribution (up to the presence of the square of residuum):

$$\begin{aligned}\Pi_{1(b,b)} &= \int_{4m^2}^{\infty} d\omega \frac{\rho_{1(b,b)}(p^2 - m^2)}{(p^2 - \omega + i\epsilon)(\omega - m^2)} \\ \rho_{1(b,b)}(\omega) &= \frac{18r^2g^2}{(4\pi)^2} \sqrt{1 - \frac{4m^2}{\omega}}.\end{aligned}\tag{A.2}$$

The most general integral to be solved is similar to the above case but with the physical masses replaced by the spectral variables.

$$I(p^2) = \int d\bar{q} \frac{1}{((p+q)^2 - \alpha)(q^2 - \beta)}\tag{A.3}$$

which after the subtraction (A.4) and integration over the Feynman parameter x leads to the appropriate single-subtracted DR (A.4)

$$\begin{aligned}
 I_{1s}(p^2) &= I(p^2) - I(m^2) = \frac{1}{(4\pi)^2} \int_0^{[1]} dx \int_{\frac{m^2 x + \alpha(1-x)}{x(1-x)}}^\infty d\omega \frac{(p^2 - m^2)}{(\omega - m^2)(p^2 - \omega + i\epsilon)} \\
 &= \int_0^\infty d\omega \frac{p^2 - m^2}{(p^2 - \omega + i\epsilon)} \frac{B(\alpha, \beta; \omega)}{(4\pi)^2(\omega - m^2)}
 \end{aligned} \tag{A.4}$$

where the function $B(u, v; \omega)$ is defined through the Khallen triangle function λ as

$$\begin{aligned}
 B(u, v, \omega) &= \frac{\lambda^{1/2}(u, \omega, v)}{\omega} \Theta(\omega - (\alpha^{\frac{1}{2}} + \beta^{\frac{1}{2}})^2) \\
 \lambda(u, \omega, v) &= (u - \omega - v)^2 - 4\omega v \\
 &= \omega^2 + u^2 + v^2 - 2\omega v - 2\omega u - 2uv.
 \end{aligned} \tag{A.5}$$

It can easily be checked that $B(m^2, m^2; \omega) = \sqrt{1 - \frac{4m^2}{\omega}} \Theta(\omega - 4m^2)$ which has already been introduced in (A.2).

The OSR scheme requires additional subtraction which is finite and henceforth can proceed by making a simple algebra

$$\begin{aligned}
 I_{2s}(p^2) &= I_{1s}(p^2) - \left. \frac{d}{dp^2} \right|_{p^2=m^2} I_{1s}(p^2) \\
 &= \frac{1}{(4\pi)^2} \int_0^\infty d\omega \frac{(p^2 - m^2)^2}{(\omega - m^2)^2(p^2 - \omega + i\epsilon)} B(\alpha, \beta; \omega).
 \end{aligned} \tag{A.6}$$

To summarize the results, we see that MMS self-energy satisfies single-subtracted DR with the absorptive part $\pi\rho_1$ given as

$$\begin{aligned}
 \rho_{\pi_1}(\omega) &= \rho_{1(b,b)}(\omega) + 2\rho_{1(b,s)}(\omega) + \rho_{1(s,s)}(\omega) \\
 \rho_{1(b,b)}(\omega) &= \frac{18r^2 g^2}{(4\pi)^2} \sqrt{1 - \frac{4m^2}{\omega}} \\
 \rho_{1(b,s)}(\omega) &= \int_{9m^2}^\infty d\alpha \frac{18r g^2}{(4\pi)^2} B(\alpha, m^2; \omega) \sigma(\alpha) \\
 \rho_{1(s,s)}(\omega) &= \int_{16m^2}^\infty d\alpha d\beta \frac{18g^2}{(4\pi)^2} B(\alpha, \beta; \omega) \sigma(\alpha) \sigma(\beta)
 \end{aligned} \tag{A.7}$$

while the self-energy in OSR scheme satisfies the double-subtracted DR with the absorptive part $\pi\rho_2$

$$\begin{aligned}
 \rho_{\pi_2}(\omega) &= \rho_{2(b,b)}(\omega) + 2\rho_{2(b,s)}(\omega) + \rho_{2(s,s)}(\omega) \\
 \rho_{2(b,b)}(\omega) &= \frac{18g^2}{(4\pi)^2} \sqrt{1 - \frac{4m^2}{\omega}} \\
 \rho_{2(b,s)}(\omega) &= \int_{9m^2}^\infty d\alpha \frac{18g^2}{(4\pi)^2} B(\alpha, m^2; \omega) \sigma_2(\alpha) \\
 \rho_{2(s,s)}(\omega) &= \int_{16m^2}^\infty d\alpha d\beta \frac{18g^2}{(4\pi)^2} B(\alpha, \beta; \omega) \sigma_2(\alpha) \sigma_2(\beta).
 \end{aligned} \tag{A.8}$$

Appendix B. Two-loop skeleton self-energy dispersion relation

The finite two-loop integral appears after the substitution of the vertex (11) to the self-energy formula

$$\int d\bar{q} d\bar{k} [(k^2 - \alpha_1 + i\epsilon)((p+k)^2 - \alpha_2 + i\epsilon)((k-q)^2 - \alpha_3 + i\epsilon) \times (q^2 - \alpha_4 + i\epsilon)((p+q)^2 - \alpha_5 + i\epsilon)]^{-1} \quad (\text{B.1})$$

where all the irrelevant pre-factors are omitted for purpose of the brevity. They will be correctly added at the end of the calculation for both renormalization schemes separately. The contribution is ultraviolet finite therefore we first calculate the unrenormalized result. Firstly, we parametrize the off-shell vertex by matching the first three denominators and consequently we integrate over the triangle loop momentum k

$$\begin{aligned} & \int \bar{k} [(k^2 - \alpha_1 + i\epsilon)((p+k)^2 - \alpha_2 + i\epsilon)((k-q)^2 - \alpha_3 + i\epsilon)]^{-1} \\ &= \int \bar{k} \int_0^1 dx dy 2y [k^2 xy + (p+k)^2(1-x)y + (k-q)^2(1-y) \\ & \quad - \alpha_1 xy - \alpha_2(1-x)y - \alpha_3(1-y) + i\epsilon]^{-3} \\ &= \int_0^1 \frac{dx dy y}{(4\pi)^2} [p^2(1-x)y(1-(1-x)y) + q^2 y(1-y) + 2pq(1-x)y(1-y) \\ & \quad - \alpha_1 xy - \alpha_2(1-x)y - \alpha_3(1-y) + i\epsilon]^{-1}. \end{aligned} \quad (\text{B.2})$$

Next, we substitute $x \rightarrow 1-x$ and after some algebra we obtain for equation (B.2)

$$\int_0^1 \frac{dx dy}{(4\pi)^2(1-y)} \left[q^2 + 2pqx + p^2 \frac{x(1-x)y}{(1-y)} - O_{1-3} + i\epsilon \right]^{-1} \quad (\text{B.3})$$

where we have used short notation $O_{1-3} = \alpha_1 \frac{1-x}{1-y} + \alpha_2 \frac{x}{1-y} + \alpha_3 \frac{1}{y}$. We continue by matching equation (B.3) with two spare denominators in equation (B.1) by using Feynman variables z and u for denominators with α_4 and α_5 , respectively. Then we can write for equation (B.1)

$$\begin{aligned} & \int d\bar{q} \int_0^1 \frac{dx dy dz du 2u}{(4\pi)^2(1-y)} \left[q^2 + 2pqxz u + 2pq(1-u) \right. \\ & \quad \left. + p^2 \frac{(1-xy)xzu}{(1-y)} + p^2(1-u) - O_{1-5} + i\epsilon \right]^{-3} \end{aligned} \quad (\text{B.4})$$

where we have used shorthand notation $O_{1-5} = O_{1-3}zu + \alpha_4(1-z)u + \alpha_5(1-u)$. Shifting $q + p(xzu + 1-u) \rightarrow q$ and integrating over new q yields

$$\begin{aligned} & \int_0^1 \frac{dx dy dz du}{(4\pi)^4(1-y)F(x,y,z)} \frac{1}{\left[p^2 - \frac{O_{1-5}}{F(x,y,z)} + i\epsilon \right]} \\ & F(x,y,z) = 1-u + \frac{(1-xy)xzu}{(1-y)} - (xzu + (1-u))^2. \end{aligned} \quad (\text{B.5})$$

Next, we substitute $u \rightarrow \omega$ where $\omega = O_{1-5}/F(x,y,z)$. Using the notation

$$\omega = \frac{ua_1 + a_2}{u^2 b_1 + ub_2} \quad (\text{B.6})$$

$$\begin{aligned}
 a_1 &= (\alpha_1(1-x)y + \alpha_2xy + \alpha_3(1-y))z + (\alpha_4(1-z) - \alpha_5)y(1-y) \\
 a_2 &= \alpha_5y(1-y) \\
 b_1 &= -(1-xz)^2y(1-y) \\
 b_2 &= (1-2xz)y(1-y) + (1-xy)xyz
 \end{aligned}
 \tag{B.7}$$

we can write the appropriate DR for equation (B.1)

$$\begin{aligned}
 \Omega(\omega; \alpha_1, \dots, \alpha_5) &= \int_0^\infty \frac{d\omega}{p^2 - \omega + i\epsilon} \int_0^1 \frac{dx dy dz}{(4\pi)^4(1-y)} \frac{\Theta(\omega - \frac{a_1+a_2}{b_1+b_2})\Theta(D)}{[\frac{\alpha_5}{U^2} - \omega(1-xz)^2]} \\
 U &= \frac{-B + \sqrt{D}}{2A} \quad D = B^2 - 4AC \quad A = \omega b_1 \quad B = \omega b_2 - a_1 \quad C = -a_2.
 \end{aligned}
 \tag{B.8}$$

Note here that the spectral function (everything after the first fraction in equation (B.8)) is always positive for allowed values of α and it is regular function of its argument ω . The various subthresholds are then given by the values of Lehmann variables α in accordance with the step function presented, noting that the perturbative threshold is given again by $4m^2$ and in that case the result is partially simplified. For completeness we reviewed the associated simplifications, namely $a_1 = m^2z(1-y(1-y))$; $a_2 = m^2y(1-y)$. Performing single subtraction for the MMS and double subtraction for OSR scheme we can recognize that the appropriate skeleton DR for master diagram has the absorptive part

$$\rho_1^{[2]}(\omega) = \frac{(6g)^4}{2} \prod_{i=1}^5 \int d\alpha_i \tilde{\sigma}(\alpha_i) \Omega(\omega, \alpha_1, \dots, \alpha_2)
 \tag{B.9}$$

for the MMS scheme and

$$\rho_2^{[2]}(\omega) = \frac{(6g_2)^4}{2} \prod_{i=1}^5 \int d\alpha_i \tilde{\sigma}_2(\alpha_i) \Omega(\omega, \alpha_1, \dots, \alpha_2)
 \tag{B.10}$$

for the OSR scheme, respectively. In fact, it gives rise to 28 various contributions to $\rho^{[2]}$ (only 12 are actually topologically independent, distinguished by the number of continuous Lehmann weights with the appropriate position of spectral variable in Ω). All of these have been found numerically for the purpose of the DSE solution.

References

[1] Salam A 1963 *Phys. Rev.* **130** 1287
 [2] Delbourgo R 1979 *Nuovo Cimento* **49** 484
 [3] Delbourgo R and Thompson G 1982 *J. Phys. G* **8** L185
 [4] Delbourgo R and Zhang R B 1984 *J. Phys. A* **17** 3593
 [5] Cornwall J M, Jackiw R and Tomboulis E T 1974 *Phys. Rev. D* **10** 2428
 [6] Schweber S S 1969 *An Introduction to Relativistic Quantum Field Theory* (Evanston, IL: Row, Peterson and Co)
 [7] Roberts C D and Williams A G 1994 *Prog. Part. Nucl. Phys.* **33** 477
 [8] Collins J C 1984 *Renormalization* (Cambridge: Cambridge University Press)
 [9] Celmaster W and Sivers D 1981 *Phys. Rev. D* **23** 227
 [10] Šauli V 2003 *J. High. Energy Phys.* JHEP02(2003)001 (Preprint hep-ph/0209046)
 [11] Baym G 1960 *Phys. Rev.* **117** 886
 [12] Cornwall J M 1997 *Phys. Rev. D* **55** 6209
 [13] Cornwall J M 1995 *Phys. Rev. D* **52** 6074
 [14] Delbourgo R, Elliott D and McAnally D 1997 *Phys. Rev. D* **55** 5230

-
- [15] Broadhurst D J and Kreimer D 2001 *Nucl. Phys. B* **600** 403
 - [16] Ahlig S and Alkofer R 1999 *Ann. Phys., NY* **275** 113
 - [17] Nieuwenhuis T and Tjon J A 1996 *Few Body Syst.* **21** 167
 - [18] Rosenfelder R and Schreiber A W 1996 *Phys. Rev. D* **53** 3337
 - [19] Rosenfelder R and Schreiber A W 1996 *Phys. Rev. D* **53** 3354
 - [20] Polchinski J 1984 *Nucl. Phys. B* **231** 269
 - [21] Morris T R 1994 *Int. J. Mod. Phys. A* **9** 2411
 - [22] Itzykson C and Zuber J B 1980 *Quantum Field Theory* (New York: McGraw-Hill)
 - [23] Detmold W 2003 *Phys. Rev. D* **67** 085011
 - [24] Šauli V and Adam J 2003 *Phys. Rev. D* **67** 044304
 - [25] t'Hooft G and Veltman M J G 1972 *Nucl. Phys. B* **44** 189
 - [26] Grunberg G 1984 *Phys. Rev. D* **29** 2315
 - [27] Fischer J 1997 *Int. J. Mod. Phys. A* **12** 3625
 - [28] Schreiber A W, Sizer T and Williams A G 1998 *Phys. Rev. D* **58** 125014